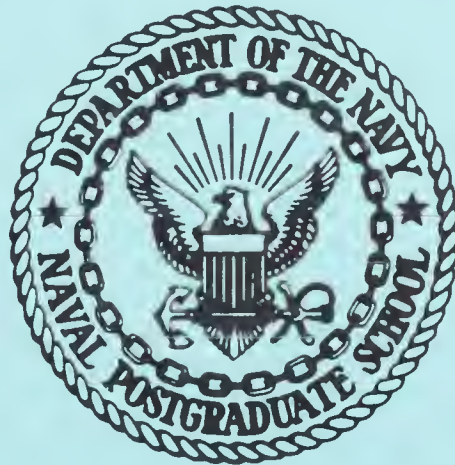


NPS ARCHIVE
1969
HALL, E.

A SENSOR INTERFACE SYSTEM
FOR DIGITAL RADIOSONDES

Eugene Mallory Hall

United States Naval Postgraduate School



THESIS

A SENSOR INTERFACE SYSTEM
FOR DIGITAL RADIOSONDES

by

Eugene Mallory Hall

December 1969

This document has been approved for public release and sale; its distribution is unlimited.

T133551

A Sensor Interface System for Digital Radiosondes

by

Eugene Mallory Hall
Lieutenant Commander, United States Navy
B.S.E.E., Purdue University, 1961

Submitted in partial fulfillment of the
requirements for the degree of

MASTER OF SCIENCE IN ELECTRICAL ENGINEERING

from the
NAVAL POSTGRADUATE SCHOOL
December 1969

ABSTRACT

A new radiosonde is needed to increase the accuracy, reliability, and speed of processing of upper-atmosphere observations. Two previous theses have investigated a pulse-modulated transmitter and more accurate sensors. This thesis proposes a method of combining the two into a workable radiosonde. Solid-state technology is used throughout including MOS integrated circuits, linear integrated circuits, and a silicon pressure transducer. System tests conducted under environmental conditions indicate satisfactory results.

TABLE OF CONTENTS

	Page
I. INTRODUCTION -----	11
II. SYSTEM DESIGN CONSIDERATIONS -----	14
III. DETAILED DESIGN CONSIDERATIONS -----	17
A. OVERALL REQUIREMENTS -----	17
B. PRESSURE INTERFACE -----	18
C. HUMIDITY INTERFACE -----	20
D. TEMPERATURE INTERFACE -----	25
E. REFERENCE VOLTAGE -----	28
IV. SYSTEM ENVIRONMENTAL TESTING -----	29
A. TEST PROCEDURES -----	29
B. INTERFACE TEST RESULTS -----	30
C. SYSTEM ENVIRONMENTAL TESTS -----	32
V. CONCLUSION -----	45
BIBLIOGRAPHY -----	48
INITIAL DISTRIBUTION LIST -----	49
FORM DD 1473 -----	51

LIST OF TABLES

	Page
I. Transmitter Characteristics -----	14
II. Sensor Characteristics -----	15
III. Simulated Humidity Sensor -----	38

LIST OF ILLUSTRATIONS

Figure	Page
1. Expected Meteorological Environment-----	12
2. Radiosonde Block Diagram -----	13
3. VCM Input Circuit -----	17
4. Constant-Current Source for Pressure Bridge -----	19
5. Pressure Amplifier Circuit -----	19
6. Humidity Logarithmic Amplifier Circuit -----	22
7. V_{BE} vs R_X at 25°C -----	23
8. Junction Voltage as a Function of Temperature ---	27
9. Temperature Amplifier Circuit -----	27
10. Reference Voltage Circuit -----	28
11. Output Voltage of Wheatstone Bridge Pressure Sensor -----	33
12. No-Load Output Voltage of Pressure Channel-----	34
13. No-Load Output Voltage of Humidity Channel -----	35
14. No-Load Output Voltage of Temperature- Compensated Humidity Channel -----	36
15. No-Load Output Voltage of Temperature Channel ---	37
16. Pressure Channel Environmental Test. VCM Frequency vs Temperature -----	40
17. Pressure Channel Environmental Test. VCM Frequency vs Pressure -----	41
18. Humidity Channel Environmental Test. VCM Frequency vs Temperature -----	42
19. Humidity Channel Environmental Test. Frequency Difference vs Temperature -----	43
20. Temperature Channel Environmental Test. VCM Frequency vs Temperature -----	44

TABLE OF SYMBOLS AND ABBREVIATIONS

ac	alternating current
dc	direct current
f	frequency
FET	field-effect transistor
Hz	hertz
I	electrical current
IC	integrated circuit
\ln	natural logarithm
LSI	large-scale integrated circuit
ma	milliamperes
mb	millibars
mv	millivolts
MHz	megahertz
MOS	metal-oxide-silicon
q	electronic charge
T	temperature
V	volts
VCM	voltage-controlled multivibrator
$^{\circ}\text{C}$	degrees centigrade
Δ	incremental quantity
Ω	ohms

ACKNOWLEDGEMENT

The author wishes to thank Mr. J. R. Hulme and Mr. R. W. Ulrickson for making the facilities of Fairchild Semiconductors available throughout the period of preparation of this thesis. In addition, gratitude is extended to those personnel of the Engineering Applications Department of Fairchild Semiconductors who provided advice and assistance during his industrial tour.

I. INTRODUCTION

The need for an improved system for collecting daily upper-atmosphere data has been well documented. The current system relies on mechanical baroswitches and vacuum-tube transmitters whose reliability and accuracy do not recommend their retention. In addition, each require individually calibrated tapes which must be used in conjunction with a manual plotter for interpreting data. Although computer programs now exist for plotting data, the primary method of local weather plotting and observing is manual.

Present sensors used include a mechanical baroswitch, a lithium-chloride humidity element, and a thermistor temperature element. Pressure changes cause a mechanical commutator to switch in the temperature, humidity, or reference data channels. The pressure is determined by counting the number of changes (clicks). There is no continuous flow of data from all sensors. Corbeille [Ref. 1], found very little correlation in data transmitted by two identical radiosondes attached to the same balloon.

An ideal system would consist of an all-solid-state state system, factory-calibrated to one standard, and with an output directly compatible with a digital computer. This system would, of course, have to be inexpensive enough to be expendable. The reliability and close manufacturing tolerance of modern semiconductor technology should make these requirements realizable. Dowell [Ref. 2] and Sagerian [Ref. 3] in

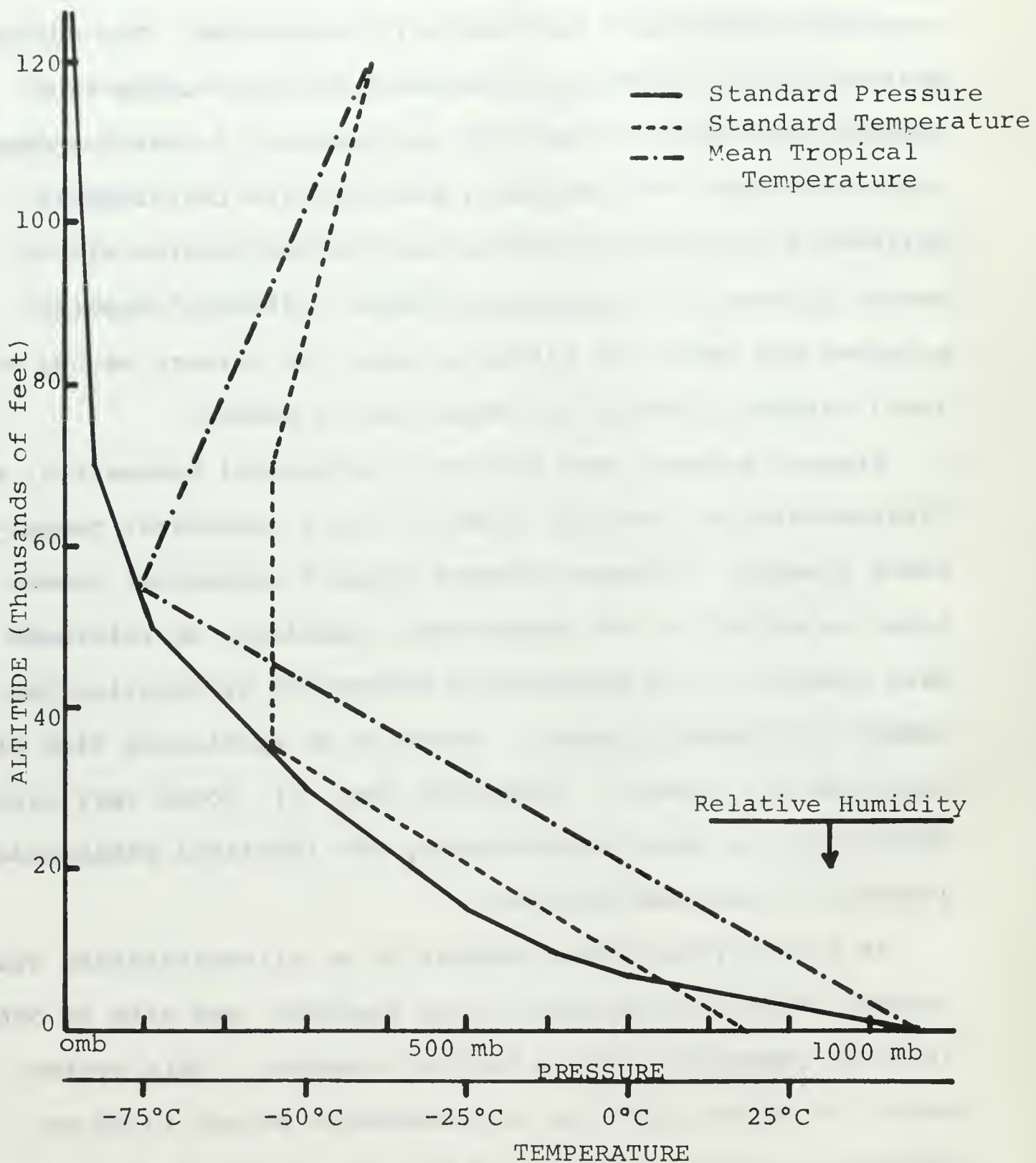


Figure 1. Expected Meteorological Environment

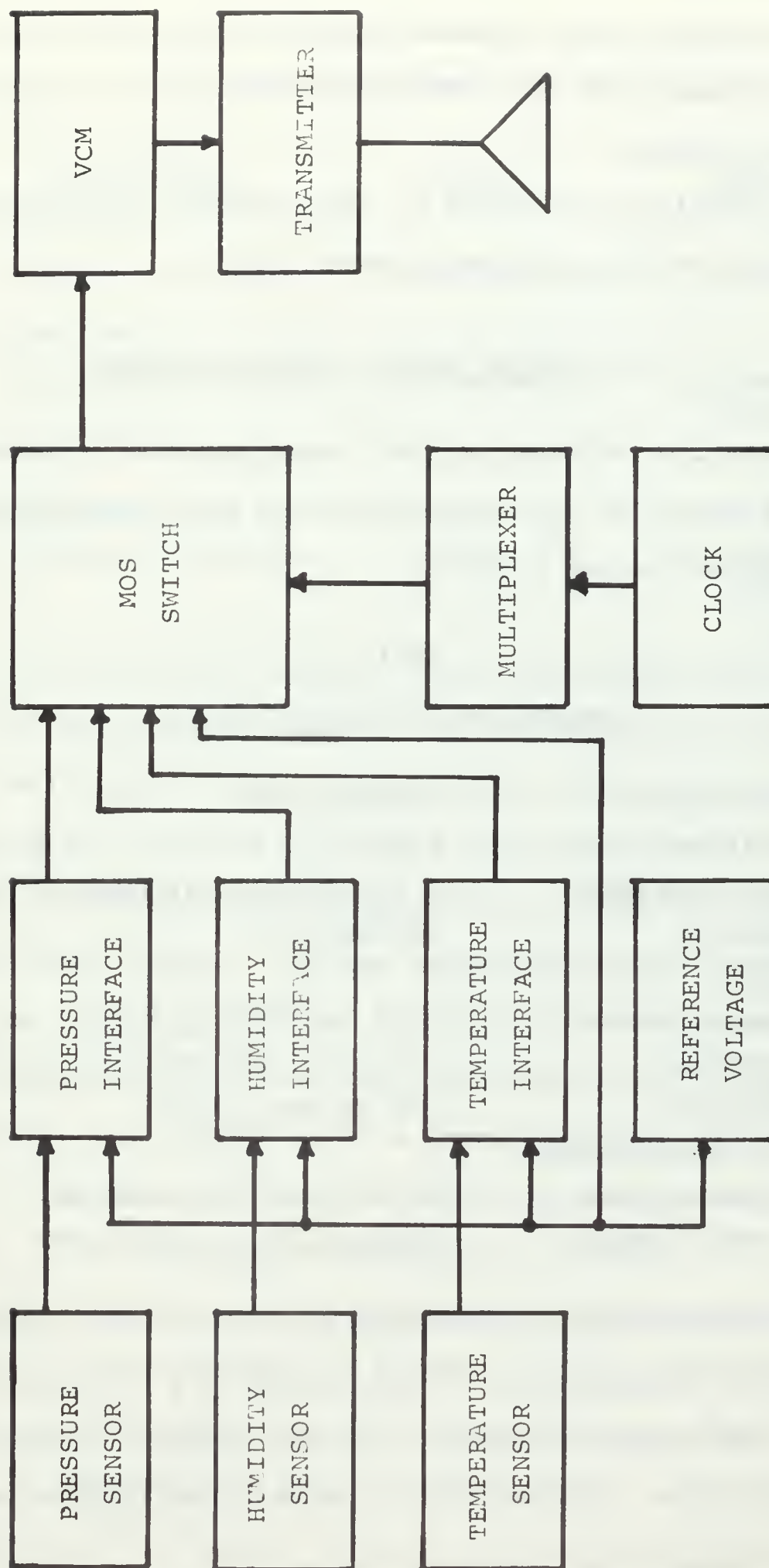


Figure 2. Radiosonde Block Diagram

previous theses have proposed transmitters which are realizable. Newcomb [Ref. 4] conducted an extensive evaluation of available sensors.

This thesis is directed to the problem of interfacing the new sensors to the proposed transmitter.

II. SYSTEM DESIGN CONSIDERATIONS

As a method of defining the interface design parameters, a brief outline of the transmitter and most promising sensors are listed in Tables I and II.

Table I

Transmitter Characteristics

Power Output	6 watts peak
Modulation	Pulse
Channel Capacity	6 (including calibration channel)
Frequency	400-403 MHz
Accuracy:	
Temperature	70°C to -70°C \pm 0.1°C
Pressure	1060 to 5 millibars \pm 1 millibar
Humidity	10% to 90% \pm 0.1%
Input Requirements:	
Primary Power	27 volts at 0.4 amperes
Data Format	Analog, -5 to -10 volts

The pressure-sensing bridge is available with passive temperature compensation. When driven by a constant-current source, the output voltage is linear, though slightly temperature sensitive. Ultimately, uncompensated bridges could be used and temperature compensation applied at a computer data reduction center.

Table II
Sensor Characteristics

<u>Parameter</u>	<u>Range</u>	<u>Output</u>
Pressure:		
Silicon Bridge	0 to 1060 + mb	0 to 150 mv
Temperature:		
Thermistor	-70°C to 70°C	Various resistance range
Silicon Junction	-70°C to 50°C	0.5 to 0.9 volts
Humidity:		
Barium Flouride	10% to 90%	20 megohms to 5 kilohms

Of all humidity sensors evaluated by Newcomb [Ref. 4], the barium flouride element was considered the most promising. The resistance of the element varied logarithmically between 10% and 90% relative humidity. The resistance at 0% relative humidity varied less than 1% over the required temperature range. Further temperature tests were not made because of the difficulty in controlling both temperature and humidity simultaneously. Elements of this type are presently not available from commercial manufacturers; however, they have been manufactured for evaluation by Jones [Ref. 5] of the National Bureau of Standards.

The thermistor is an inexpensive temperature-sensing device. The parameter of interest is the resistance of the unit. A wide selection of dynamic range and resistance at 25°C is available in many configurations. One manufacturer offers a line of epoxy-coated, precision, matched thermistors

which seem promising. The temperature accuracy is guaranteed to $\pm 0.2^{\circ}\text{C}$ between $+70^{\circ}\text{C}$ and -20°C , however, below this temperature range the accuracy decreases to $\pm 1^{\circ}\text{C}$ at -80°C . The resistance variation of these devices is generally logarithmic, but for the accuracy specified in Table I, computer compensation would be required. Their greatest advantage is consistency between units. Thermistors are available with resistances that vary over the same range as that of the humidity element.

The base-emitter voltage (V_{BE}) of an ordinary transistor when operated in the common-base configuration is a linear function of temperature. All semiconductor diodes exhibit a similar effect. An investigation will also be made of the possibilities of using this sensor. This diode or transistor could be added to the pressure bridge chip. This process must, however, be carefully controlled so that all junctions have the same characteristics.

Although five data channels are available, only three data sources are presently planned. The reference channel must also be provided with a constant reference voltage. Figure 1 is a profile of the environment to be sensed by the radiosonde. The humidity information ceases to be of use after the first 25% of the flight, and so a third channel becomes available at this point. Ozone concentration and navigational position are two other possible data inputs, but sensors are not presently available.

III. DETAILED DESIGN CONSIDERATIONS

A. OVERALL REQUIREMENTS

All sensor channels must provide essentially a dc voltage for 50 milliseconds to the voltage-controlled multivibrator (VCM) through a metal-oxide-silicon (MOS) gate. The input-output characteristics of the individual interface channels are determined as shown in Fig. 2.

1. The output characteristics of all channels are the same.
2. The MOS switch has an ON resistance of about 250 ohms. The previously specified value of output voltage, -5 to -10 volts, is the recommended voltage range for the switch.
3. The input circuit of the VCM is a current source and is shown in Fig. 3. V_{IN} is the output of the MOS switch,

and is either ground or the -5 to -10 volt interface output. The current sources provide a current between 0.2 and 0.5 milliamperes as charging current to the capacitors. The sources have an H_{FE} of at least 200, and therefore, present a high impedance. An estimate of 4 megohms each or a combined input impedance of 2 megohms seems reasonable.

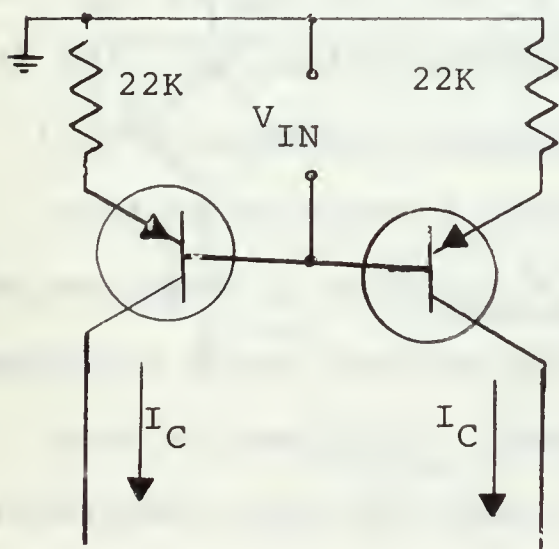


Figure 3. VCO Input Circuit.

4. Ideally, each interface circuit should be dependent only on the reference voltage and the parameter measured.

5. The clock output, a nominal -16V square wave of 20 Hertz and any multiple of this frequency 2^n , $0 \leq n \leq 14$, is also available as a driving signal.

B. PRESSURE INTERFACE

The pressure-sensing element is a silicon wheatstone bridge. When excited with 5 milliamperes of constant current, the output varies from 0 to 150 millivolts. The nominal impedance of the bridge is 2 kilohms.

Figure 4 is the general configuration for this constant-current source. Q_1 is a low-cost epoxy dual transistor. Q_{1A} is the current source. By biasing the base of Q_{1A} to provide 5 volts across R_3 , the 5-milliamper drive current is obtained. Q_{1B} is used as temperature compensation. The bias for Q_{1A} is the sum of the voltage across R_2 and the V_{BE} of Q_{1B} . As both transistors have similar characteristics, the rise in V_{BE} of both transistors with decreasing temperature will cause the bias to track and maintain a constant voltage across R_3 . The allowed error is a function of the bias network current. In order to keep the battery drain a minimum, a current of 1-milliamper was used. This results in a change in voltage of less than 1% over the full temperature range.

In order to change the level of the output voltage from 0 to 150 millivolts to -5 to -10 volts, a simple operational amplifier was used with a gain of 30. The 5-milliamper

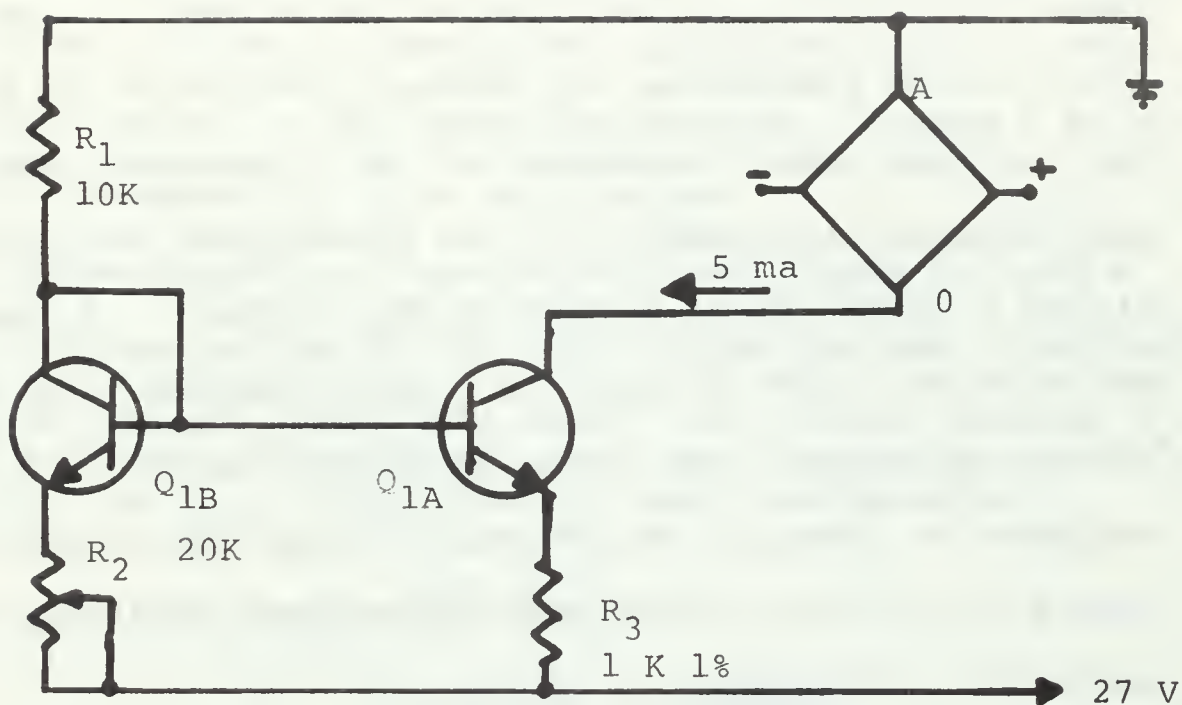


Figure 4. Constant-Current Source for Pressure Bridge

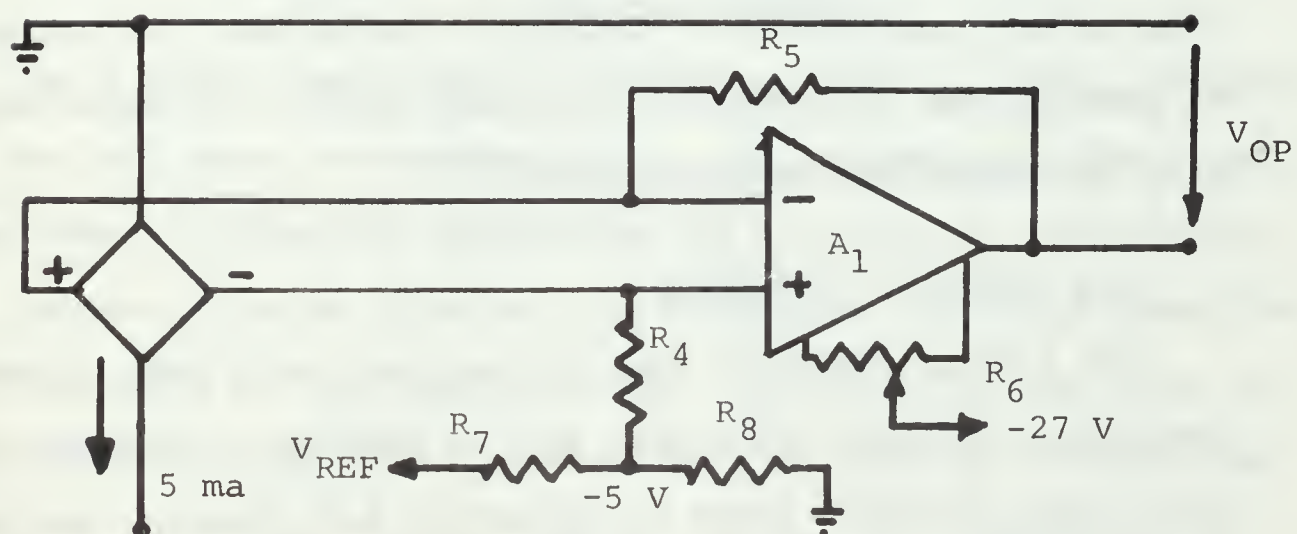


Figure 5. Pressure Amplifier Circuit

driving current has an additional advantage in this case; it causes the voltage at the arms of the bridge to vary around -5 volts and simplifies the loading problem of the bridge. The 2-kilohm output impedance of the bridge was used as the gain-determining element for the operational amplifier. Figure 5 is the final design of this circuit. R_7 and R_8 are set when the value of V_{REF} has been selected. R_6 is the offset adjustment, and is set by substituting a 2-kilohm resistor in place of the pressure bridge and adjusting the output for 0 volts across the operational amplifier input and output terminals.

A possible source of error is the use of the bridge impedance as a gain-determining element. The actual value of the resistance may change between units and has a positive temperature coefficient. This will cause gain to increase as temperature decreases. The exact effect of these factors will be determined experimentally.

C. THE HUMIDITY INTERFACE

The barium-fluoride humidity sensor was found to vary in resistance between 5 kilohms and 20 megohms. Various passive resistance networks were investigated and found to be insensitive at one extreme range or the other. It was decided that an amplifier with a logarithmic response was needed. An additional problem exists in that the element becomes polarized when driven by a dc source so that an ac voltage of some sort must be used to excite the element.

A review of technical literature resulted in the selection of an arithmetic logarithmic amplifier [Ref. 6] that could be adapted to this specific problem. Figure 6 is the circuit proposed for this application.

A characteristic of operational amplifiers is that a virtual ground exists at the input terminals and a negligible amount of current flows into them. The current through R_x is then I_C . For Q_{2A} in the grounded base configuration:

$$(1) \quad V_{BE} = \frac{KT}{q} \ln \frac{I_C}{I_S}$$

K = Boltzman's constant

q = charge of an electron

T = temperature in °K

I_S = collector saturation current of the transistor.

At a given temperature, therefore, the V_{BE} of Q_{2A} depends on two currents, one depending on the unknown resistor, and the other on physical properties of the type of transistor. R_{14} prevents large fluctuations caused by the large open-loop voltage gain of the amplifier and the small voltage gain of the grounded-base configuration by limiting the closed-loop gain of the first stage. The V_{BE} of Q_{2B} is a function of I_{C2} and the same I_S as mentioned for Q_{2A} . I_{C2} is determined by R_{15} and the reference voltage and is constant for a given value of R_{14} . The input voltage to A_3 is the difference in the V_{BE} of the two transistors:

$$(2) \quad V_{in2} = V_{BEA} - V_{BEB}.$$

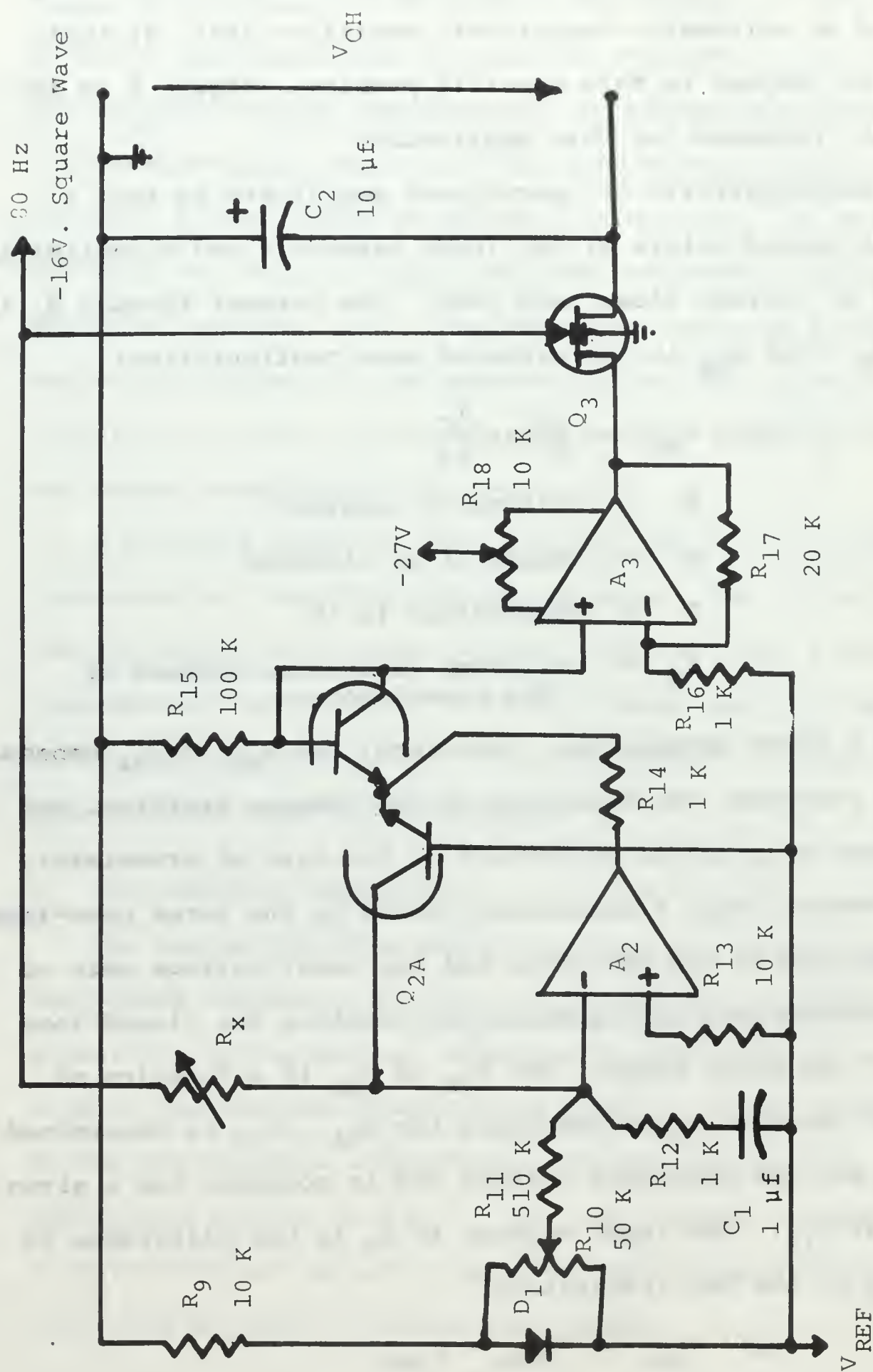


Figure 6. Humidity Logarithmic Amplifier Circuit

Substituting (1) into (2) for both transistors:

$$(3) \quad V_{IN2} = \frac{KT}{q} \ln \frac{I_{C1}}{I_S} - \frac{KT}{q} \ln \frac{I_{C2}}{I_S}.$$

Rearranging the terms of (3) results in the relation:

$$(4) \quad V_{IN3} = - \frac{KT}{q} \ln \frac{I_{C2}}{I_{C1}} = - \frac{KT}{q} \ln \frac{R_x}{R_{14}}.$$

A_3 is a standard inverting operational amplifier with gain G_3 . The output voltage is then given by equation (5).

$$(5) \quad V_O = (V_{REF} + G_3 \frac{KT}{q} \ln \frac{R_x}{R_{14}}) \text{ volts.}$$

At room temperatures, $\frac{KT}{q}$ is in the order of 25 millivolts for a decade change in resistance and $\ln 10 = 2.3$. The output voltage change is in the order of $(57 G_3)$ millivolts/decade. A five-decade change in the resistance of R_x indicates G_3 should be:

$$(6) \quad G_3 = \frac{5V}{5 \times 57 \times 10^{-3} V} = 17.$$

A value of 20 will be used for evaluation as the full 5-decade change is not required, and minor gain adjustments can be made later.

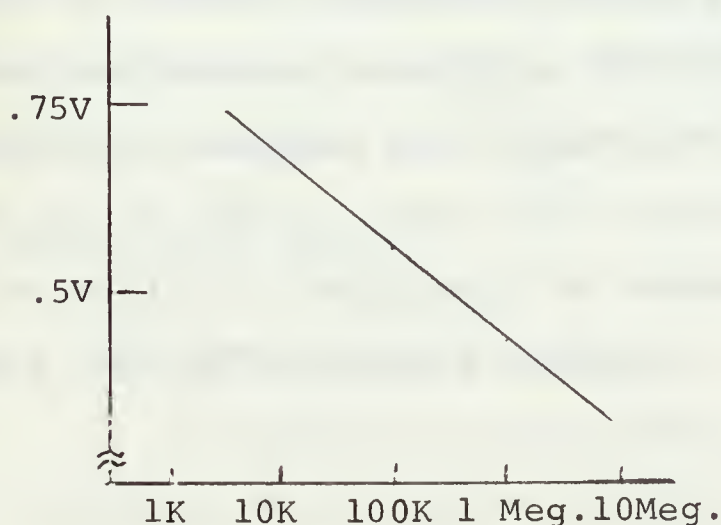


Figure 7. V_{BE} vs R_X at 25°C.

The next problem is to find the values of R_{14} and V_{REF} . In order to evaluate various transistors and obtain a general idea of the variables, several simple circuits were built and tested at various temperatures. A typical

30-milliampere transistor V_{BE} is shown in Fig. 7. As larger chip sizes are used, the curve will remain linear to lower values of resistance. The curves shift up and slightly change slope as temperature decreases.

The value of R_{14} chosen should be near the middle of the linear range. This will cause the dynamic range to shift in both directions. One hundred kilohms and one megohm are the outside bounds of the possible values in this case. V_{REF} must now be decided before an exact R_{14} is chosen.

The clock divider chain is a source of "free" ac voltage except that it is unsymmetrical with respect to ground. If, however, -8 volts should be chosen as reference, the clock output is symmetrical to this voltage. Therefore, V_{REF} is chosen primarily on this basis.

The input voltage to A_3 is the difference in base-emitter voltages and will be positive with respect to V_{REF} as R_x approaches its maximum value of 20 megohms. Twenty megohms is 2.2 decades from 100 kilohms and at 1.2 volts/decade the output voltage should be -5.3 volts. A similar calculation predicts -9.5 volts for 5 kilohms. These voltages are satisfactory and 100 kilohms will be used as the reference resistor.

In order to prevent the output from changing when the negative voltage is applied to the input, an MOS switch should be incorporated which charges or discharges C_2 only on the proper half cycle. For evaluation a modified Fairchild MOS 3705 was used.

Small additional components include the R_{12} - C_1 network which by-passes the input for high frequencies. This prevents the circuit from oscillating at large values of R_x . The bias network R_{10} - D_1 provide a bias for A_2 . The maximum bias requirements are in the order of 0.5 microamperes at 25°C and increase as the β of the input stages decrease. Transistor β decreases as temperature decreases, and this bias becomes significant with respect to I_C when R_x is large. For example, 20 megohms causes an I_C of only 0.4 microamperes. This results in an apparent increase in resistance at low temperatures. By adjusting R_{10} for a portion of the diode forward voltage, the linearity of the high-resistance range is assured over a wider span of temperatures. The diode voltage will increase at the rate of 1.6 millivolts/°C and provide increased bias with increasing temperature. An amplifier with smaller bias requirements should be used in a production model and may eliminate this need.

No offset adjustment is provided for A_2 because the offset voltage is not significant when compared to 8 volts. R_{18} is the offset adjustment for the second stage. The method of making this adjustment is to insert a 100-kilohm resistor at the R_x terminals and adjust for 0 volts between V_{REF} and V_{OH} output terminals.

D. THE TEMPERATURE INTERFACE

1. An identical logarithmic amplifier was built on the assumption that a suitable thermistor could be procured.

This was not the case, however. Problems of self heat at higher temperatures prevented accurate measurements with thermistors.

2. The V_{BE} variation with collector current was found to be quite linear in earlier investigations (See Fig. 8). If a transistor similar to Q_{2B} is used with fixed collector current and the V_{BE} amplified by an operational amplifier, a linear voltage should result. The circuit in Fig. 9 will be used. R_{20} sets the original voltage level of the junction. R_{21} and R_{22} offset this value so that V_{OT} varies above and below the reference voltage. The degree of loading is determined by the values of the input and feedback resistors. The value of gain is also determined by these resistors. For full voltage swing, the change in V_{BE} can be seen to be about 0.25 volts in Fig. 8. The value of G_4 can then be calculated:

$$5V = G_4 \Delta V_{BE}$$

$$G_4 = 20$$

This value determines the ratio of R_{23} to R_{25} and R_{24} to R_{26} to be 20. The input terminals have a nominal -7.5 volts applied. This means that when the output voltage is -5 volts, $(2.5V \div R_{25})$ amperes must flow. If R_{25} is 100 kilohms, 25 microamperes will be required. The bleeder current through R_{21} must be much larger than this to prevent loading. If 10 kilohms is chosen, then $I_1 = 800$ microamperes and this condition is satisfied. A similar condition exists at the summing terminal. Here, $V_{BE\min} = 0.5$ volts and $I_2 = 5$ microamperes. In a marginal amplifier the bias requirement could be 0.5 microamperes, which could cause a small error. As the

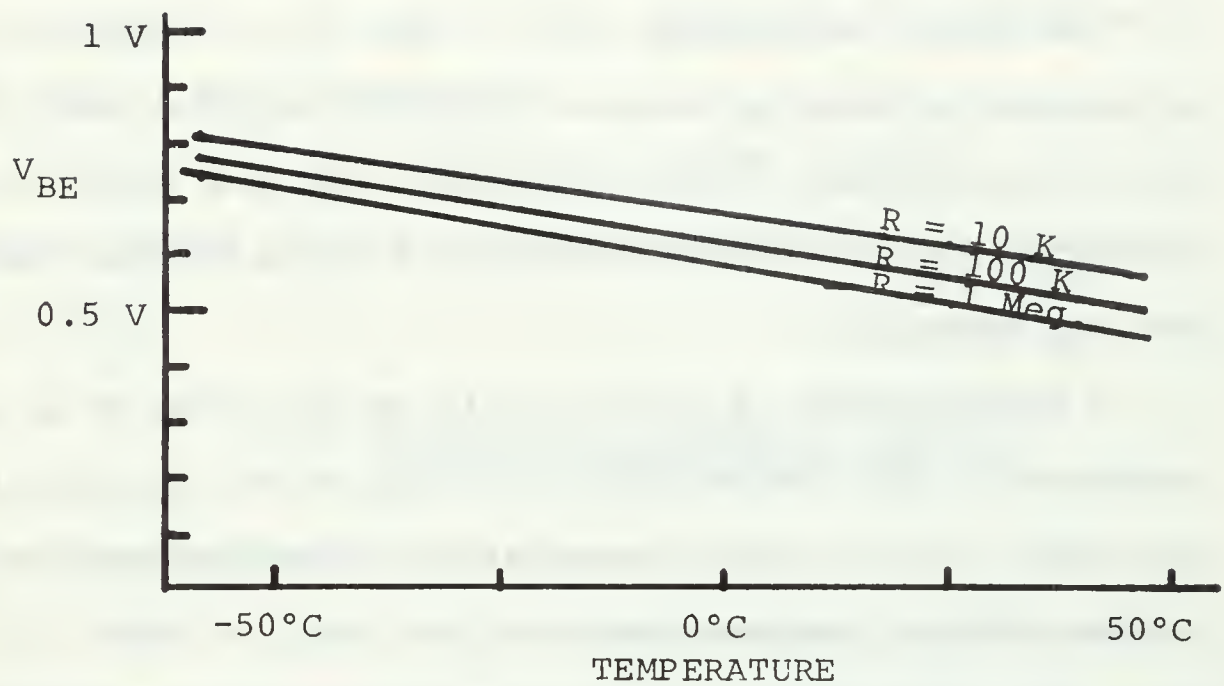


Figure 8. Junction Voltage as a Function of Temperature

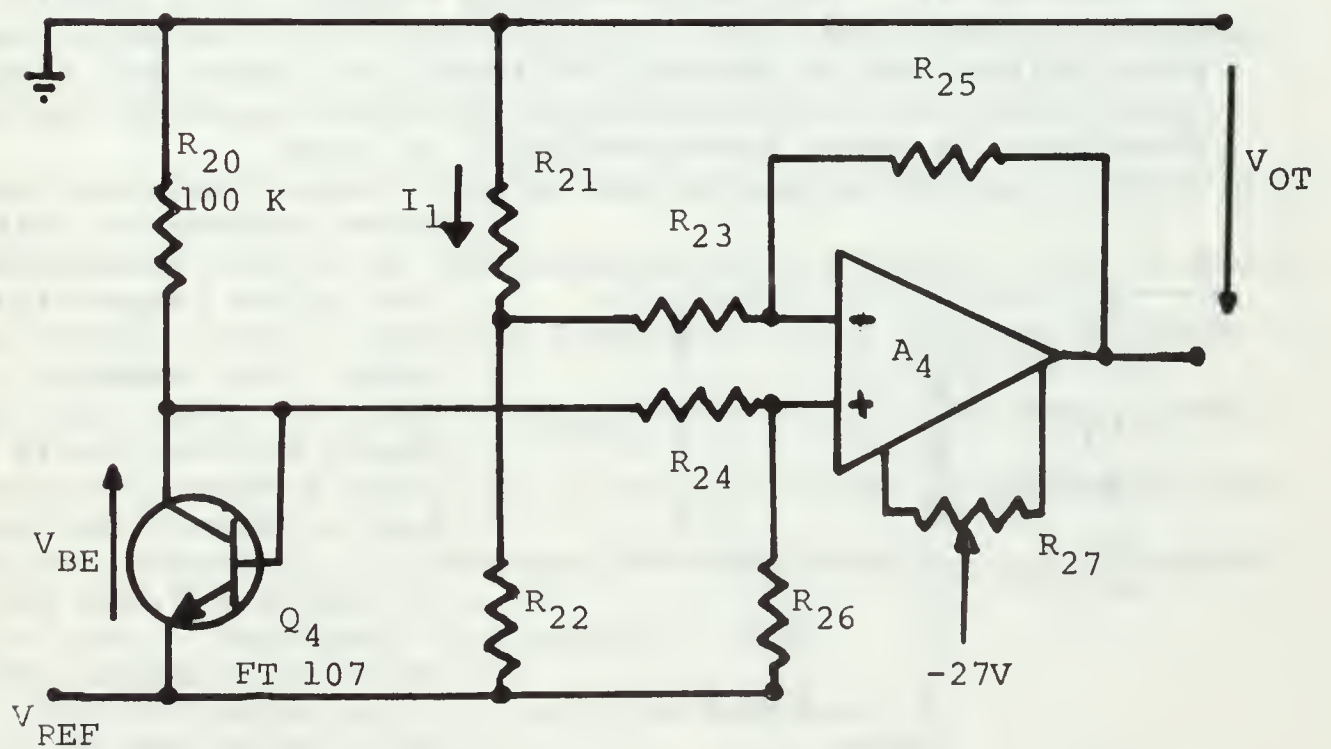


Figure 9. Temperature Amplifier Circuit

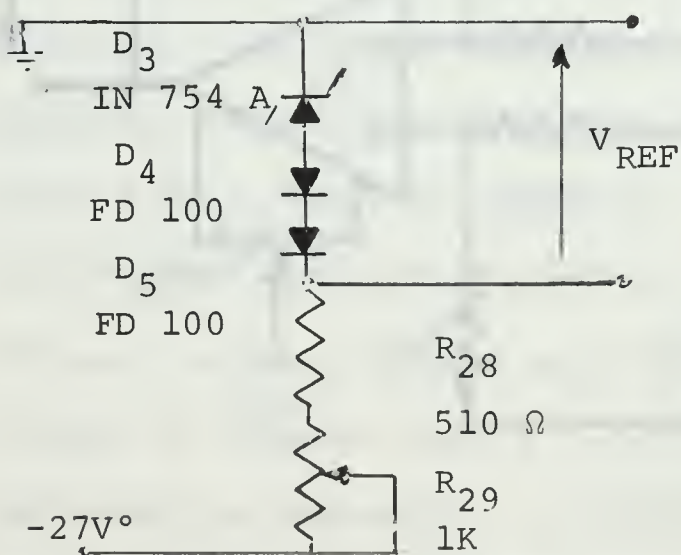
"typical" value is listed as 0.08 microamperes, it is felt that this is a safe design.

The offset adjustment R_{27} is used in this amplifier. The adjustment is made by temporarily shorting the junction of the collector-base of the transistor and the junction of R_{21} and R_{22} . R_{27} is then adjusted for 0 volts across the V_{REF} and V_{OT} terminals.

A disadvantage of this circuit is the lack of an absolute reference. This means that the slope of the output will be constant, but the local temperature at launch must be observed as the initial temperature.

E. REFERENCE VOLTAGE

Two possible sources of reference voltage were mentioned in Section II. The center-tapped battery will remain a possibility but as battery voltages are load- and temperature-dependent, a zener reference will be used.



Zener diodes as references are quite temperature sensitive. For example, a zener diode in the 8-volt range has a temperature coefficient of about + 0.06% per °C. This is a change of about 5 millivolts per °C or a total change of 0.8 volt over the limits of the operating

Figure 10. Reference Voltage Circuit.

range. A 6.8 volt zener, however can be combined with two forward-biased diodes to give a total temperature coefficient of $+ 0.2\text{mv}/^{\circ}\text{C}$. This is a total shift of 30 millivolts or 0.4% and is more acceptable.

Figure 10 is the reference voltage circuit. R_{29} is a carbon trimmer which is used to compensate for component tolerances.

IV. SYSTEM ENVIRONMENTAL TESTING

A. TEST PROCEDURES

In order to test the proposed interfacing system, a transmitter and multiplexer were connected with the interface and sensors. The characteristics of the transmitter were reported by Sagerian [Ref. 3]; therefore, the interface board was initially placed in the environmental chamber so that it alone could be characterized. Two tests were made, no-load tests in which the unloaded voltage output of each sensor amplifier was measured and a loaded test in which the outputs were connected directly to the VCM and buffer. For this test, the switching transistor for the power oscillator was removed from the circuit, and the frequency of the VCM was measured. A frequency counter and digital voltmeter were used to measure the outputs.

The following artificialities existed:

1. The VCM was not loaded.
2. The VCM was not multiplexed -- this is not considered a major factor as CW operation should be a worse case than multiplexed operation.

3. A breadboard multiplexer was used.

4. A MOSFET was used in place of the proposed gate to be included on the LSI circuit.

5. A decade resistance network was used to simulate the humidity element. This was a necessary deviation in order to characterize the logarithmic amplifier with known resistances.

Originally the system was configured with the proposed pressure circuit and two identical logarithmic amplifiers. This group of sensors was used to test the suitability of a thermistor placed directly in the humidity circuit. One logarithmic amplifier was later modified to the junction voltage-multiplier circuit described in Section III. A further modification was made by inserting a modified silicon bridge in place of R_{16} . The purpose of this change was to compensate for the decrease in input voltage to A_3 by introducing a negative temperature coefficient to the gain of A_3 .

B. INTERFACE TEST RESULTS

1. The interface circuit board and associated sensors were placed in an environmental chamber. The pressure transducer was placed in a small pressure chamber. All other components were subjected to the environment in the chamber. The reference voltage and all offset voltages were adjusted as previously described. The output voltage was measured to three significant figures using a Fairchild Model 7100A Digital Voltmeter. Data was plotted as a function of temperature and the parameter to be measured by the circuit of interest.

a. Figure 11 is a graph of the output of the pressure transducer alone. The output voltage is linear for each temperature range, but has a temperature-dependent offset. The output voltage varies 5 millivolts at either extreme of the pressure range as the temperature is varied. This is an error of $\pm 1.5\%$ at atmospheric pressure and over 100% at 5 millibars. The voltage variation is constant for all pressures, therefore the error increases as pressure is decreased. This indicates computer processing will be required to achieve the required accuracy.

b. Figure 12 is a graph of the unloaded output of the pressure amplifier. The effect of increased gain at lower temperatures is apparent. The output is linear at each temperature and varies between 4.93 mv/mb at 25°C and 5.87 mv/mb at -50°C . In itself, this is not necessarily undesirable as the VCM output frequency is known to decrease with temperature and these temperature coefficients will partially cancel each other.

c. Figure 13 is a graph of the output voltage of the humidity amplifier as a function of resistance and temperature. The change in output voltage per decade closely agrees with the predicted values, 1.3 volts/decade at 50°C and 0.85 volts/decade at -50°C . The effect of increased bias requirements is also apparent in the 20-megohm curve.

d. Figure 14 is a graph of the output of a temperature compensated humidity amplifier. The compensation is made by inserting a silicon bridge chip as R_{16} . The

resistance decreases with temperature, causing the gain to increase. The feasibility of using a silicon diffused resistor is demonstrated satisfactorily. A similar resistor specifically designed for this application should be an even greater improvement. The value of this compensation is that the sensitivity of the humidity-measuring circuit is constant over the range of temperatures.

e. Figure 15 is the response of the temperature amplifier under no-load conditions. In itself, this curve has little value except to demonstrate the feasibility of measuring temperature in this manner. Temperature is the most important parameter to be measured and the complete VCM temperature characteristic must be known for any data to be usable.

2. This group of tests successfully demonstrates that the design submitted meets the general specifications as stated in Section II except for accuracy. In all cases, computer processing will be necessary to obtain the accuracies desired. Sagerian [Ref. 3] found that a second-order equation was necessary to meet the specifications when only the VCM was considered.

C. SYSTEM ENVIRONMENTAL TESTS

1. During these tests the complete radiosonde breadboard was placed in the environmental chamber. Again, the pressure transducer was placed in the small pressure chamber and all other components were open to the environment. During these tests the VCM was connected directly to the output of the

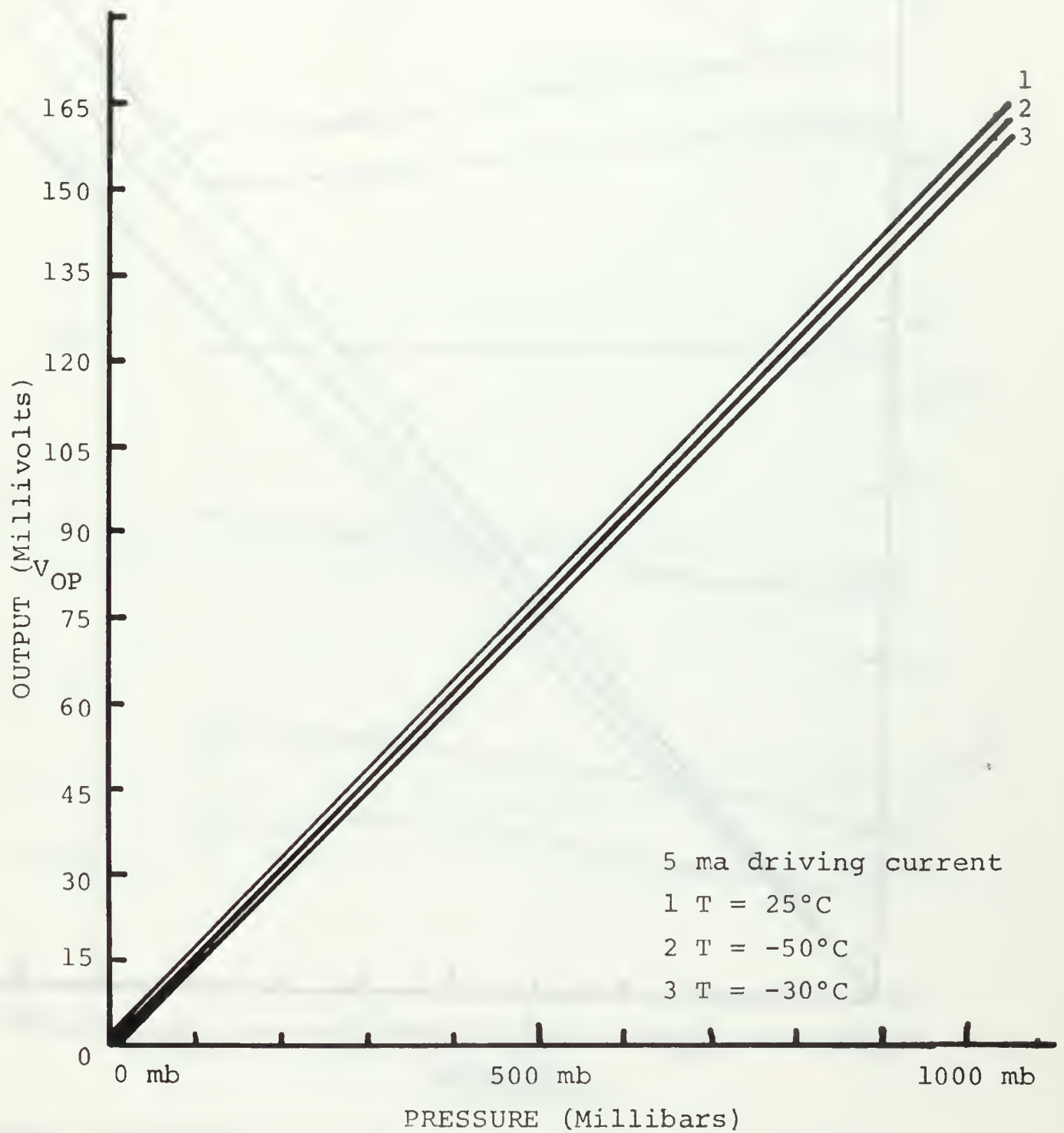


Figure 11. Output Voltage of Wheatstone Bridge Pressure Sensor.

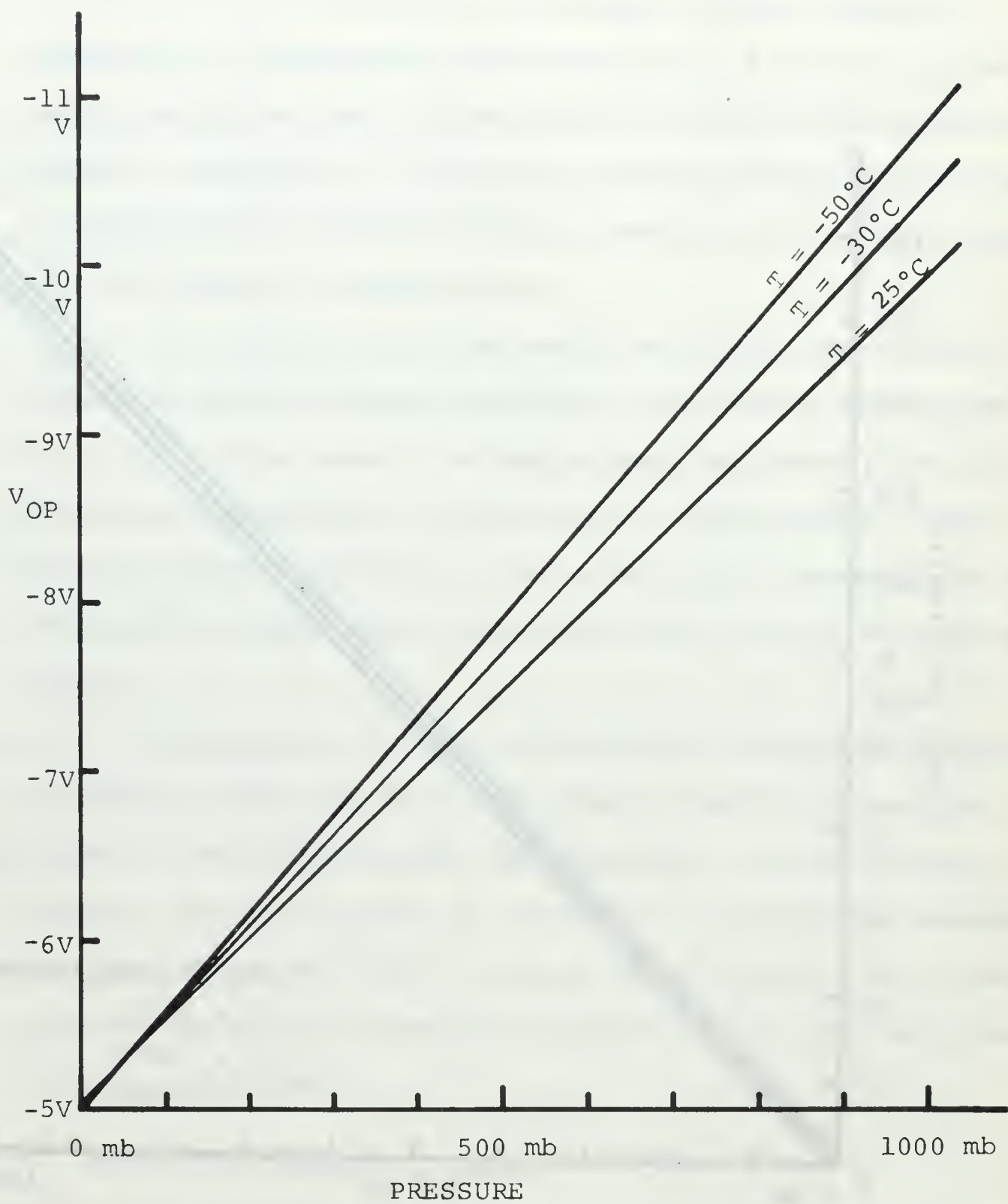


Figure 12. No-Load Output Voltage of Pressure Channel.

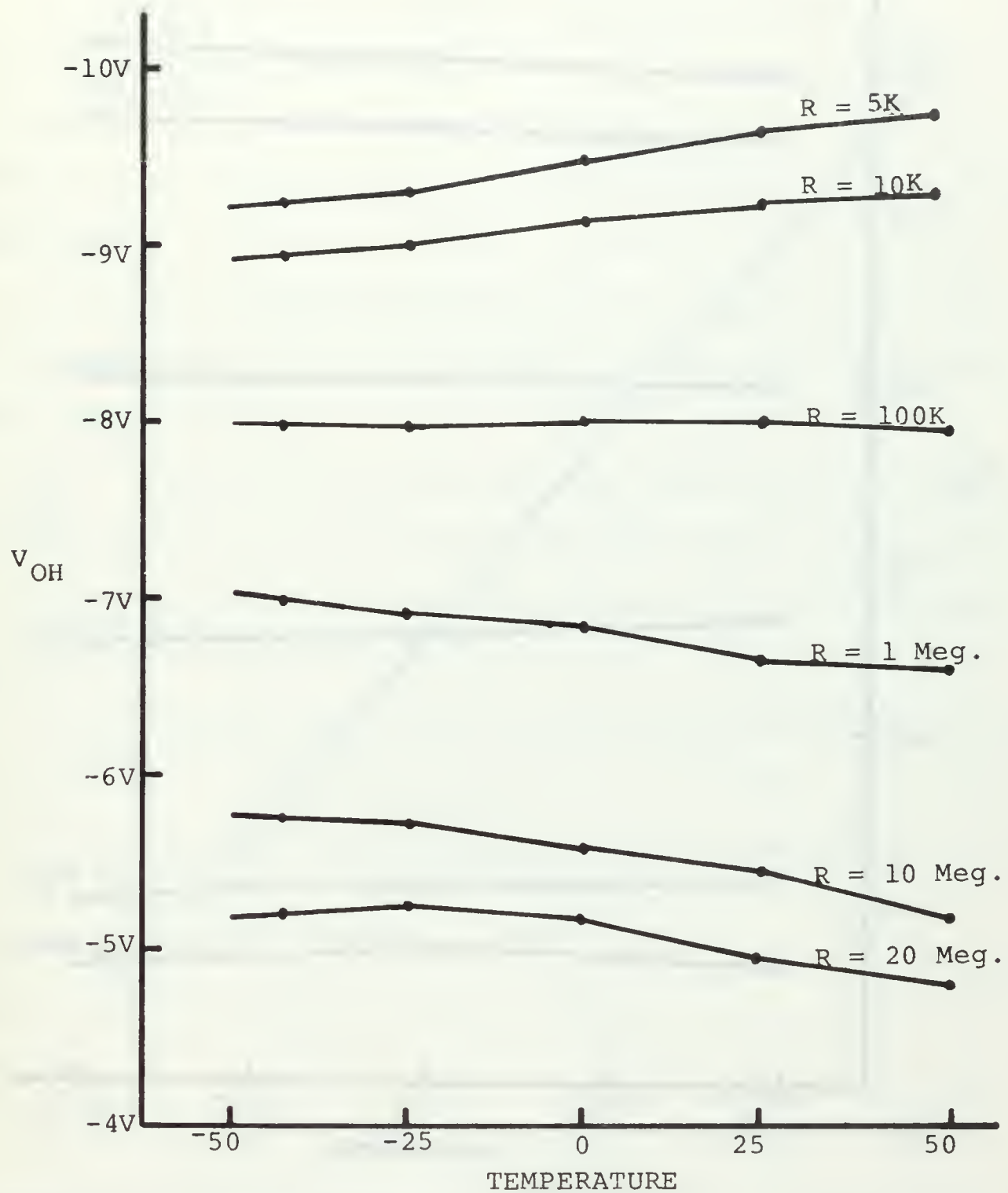


Figure 13. No-Load Output Voltage of Humidity Channel.

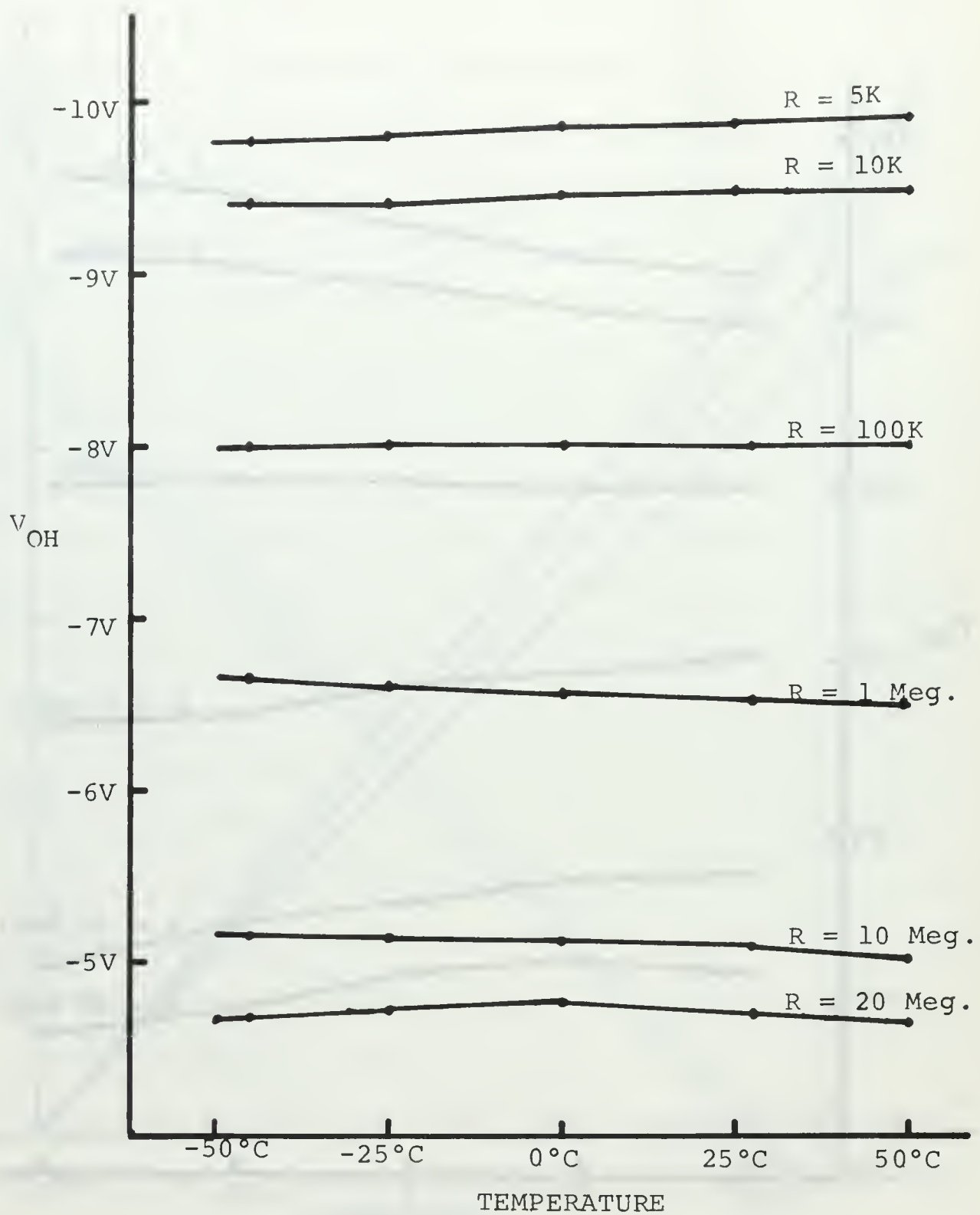


Figure 14. No-Load Output Voltage of Temperature-Compensated Humidity Channel.

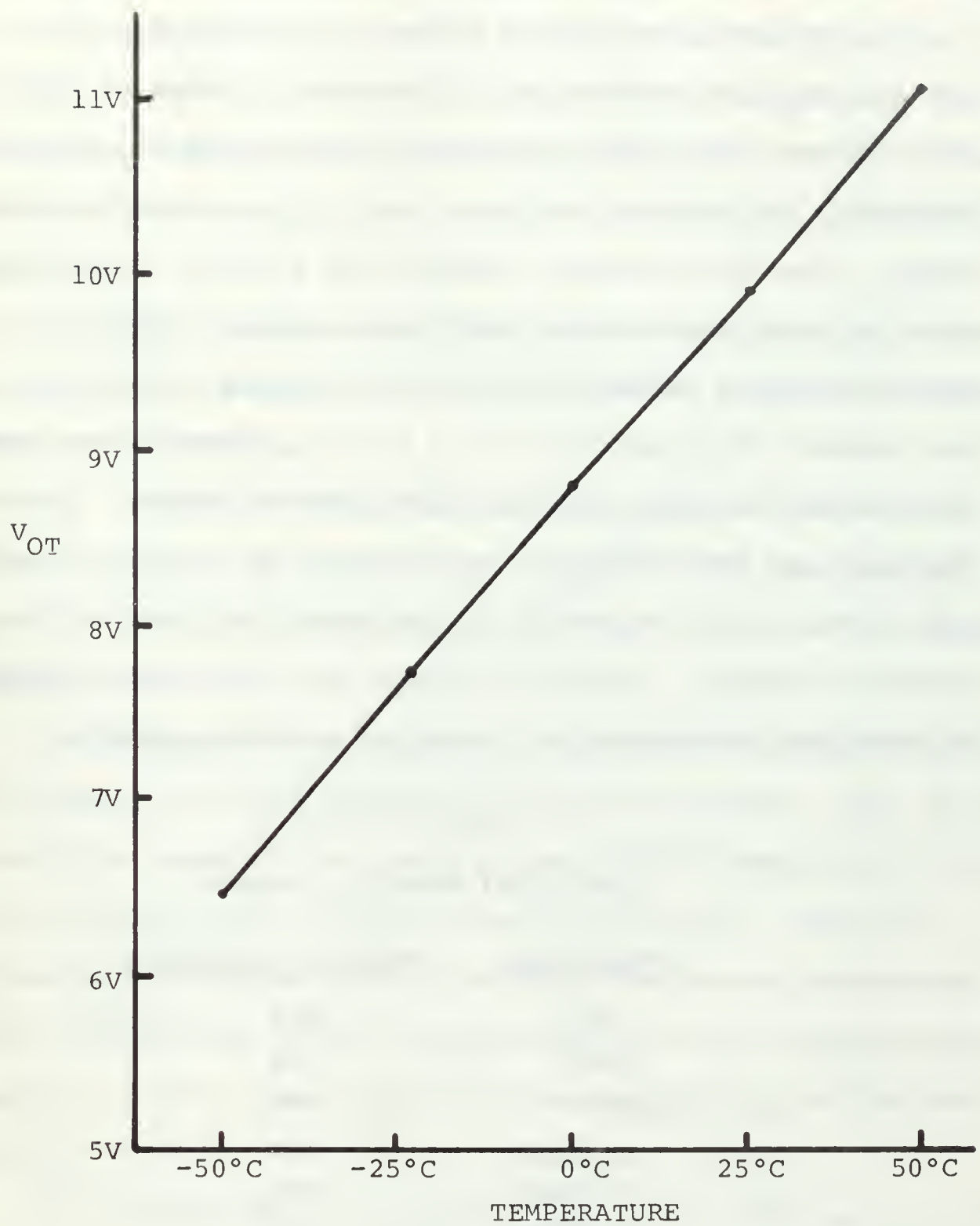


Figure 15. No-Load Output Voltage of Temperature Channel.

data channel being investigated. The output of the VCM was measured with a Hewlett-Packard Model 5247M Frequency counter.

The pressure was varied between atmospheric pressure and an absolute pressure of 100 microns, a range of 1020 to 3 millibars. The data was taken in the sequence atmospheric pressure, 100 microns, -11 psi, and -5 psi at each temperature. The environmental chamber was allowed about 30 minutes to stabilize between each temperature. Temperature was measured with a mercury thermometer exposed to the air inside the chamber to an accuracy of $\pm 0.5^{\circ}\text{F}$. Pressure was measured on a large dial-type Bourden-tube pressure gauge. Pressure readings are repeatable to an accuracy of 0.1 psi. Humidity was simulated by inserting 1% resistors in place of the humidity element. Table III lists the resistance values used to simulate corresponding values of relative humidity.

Table III
Simulated Humidity Sensor

<u>Resistance</u>	<u>Relative Humidity</u>
5K Ω	85%
10K Ω	75%
100K Ω	50%
1 Meg Ω	30%
10 Meg Ω	10%
20 Meg Ω	0%

All interface channel outputs were measured under no-load conditions and when loaded by the VCM. In addition, the reference voltage was measured and the frequency caused

by this voltage was used as the reference frequency. Results of this test are plotted and are commented upon individually.

a. Figure 16 is a graph illustrating the variation of output frequency with temperature at four pressures. The effect of the gain increase at low temperatures is evident in the levelling out of the curves in the left half of the figure.

The change in frequency over the whole temperature range varies between 1.5% at atmospheric pressure to about 10% at 100 microns.

b. Figure 17 demonstrates the effect of temperature on the linearity of the pressure channel. The relationship is not a simple one and requires much more data and a computer analysis.

c. Figure 18 is a graph illustrating variation of VCM frequency at fixed values of relative humidity. The large positive temperatures coefficient of the frequency of the VCM is quite evident at temperatures below 0°C. Figure 19, however, indicates that this effect is not so pronounced on the differences of the frequencies from the reference frequency. Both figure indicate the instability of the very high-resistance (low relative humidity) range.

d. Figure 20 is a graph of the output frequency of the temperature channel as a function of temperature. Again, the graph is not linear but indicates that this method can be used to cause the desired frequency variation over the desired temperature range.

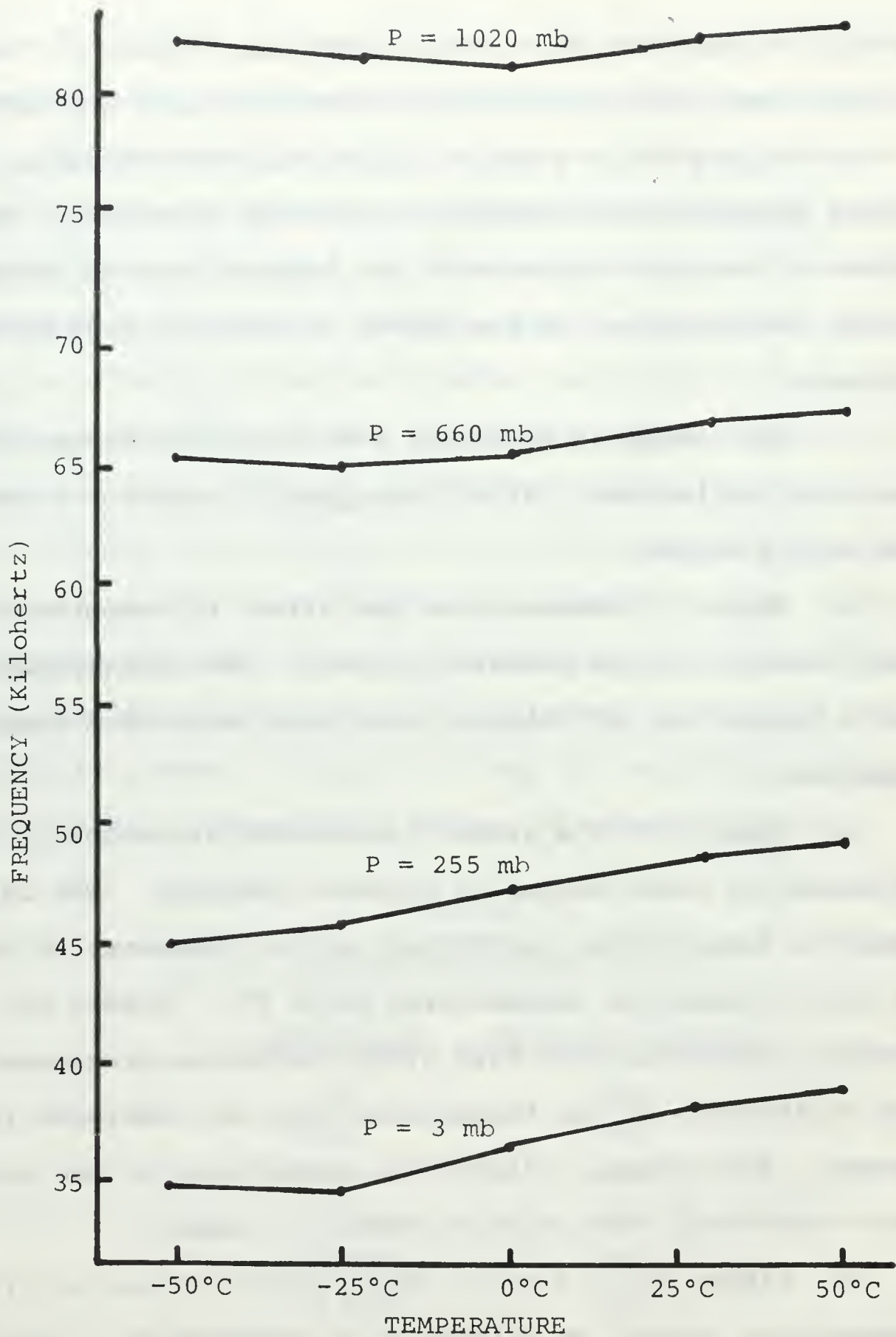


Figure 16. Pressure Channel Environmental Test VCM Frequency vs. Temperature.

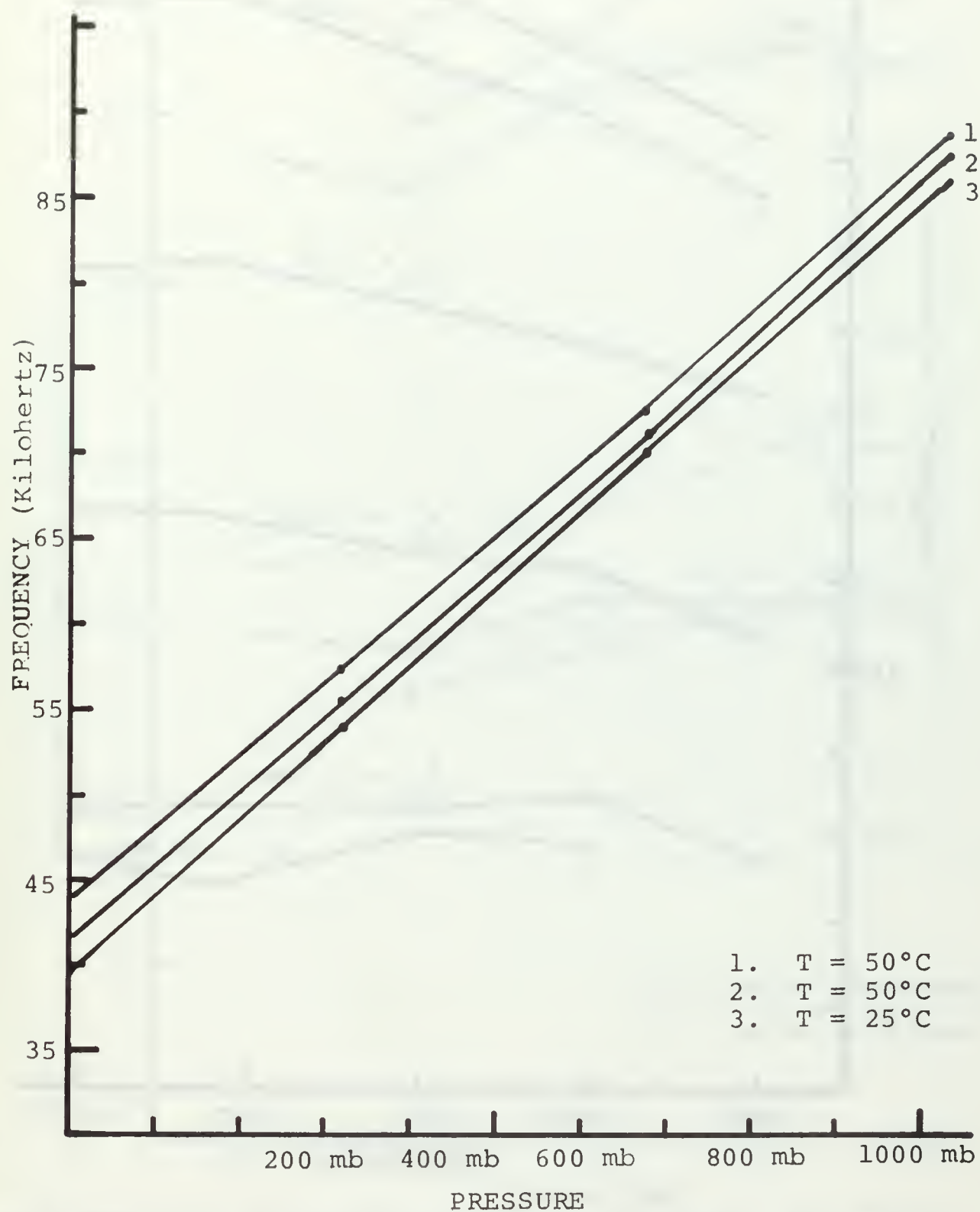


Figure 17. Pressure Channel Environmental Test VCM Frequency vs. Pressure.

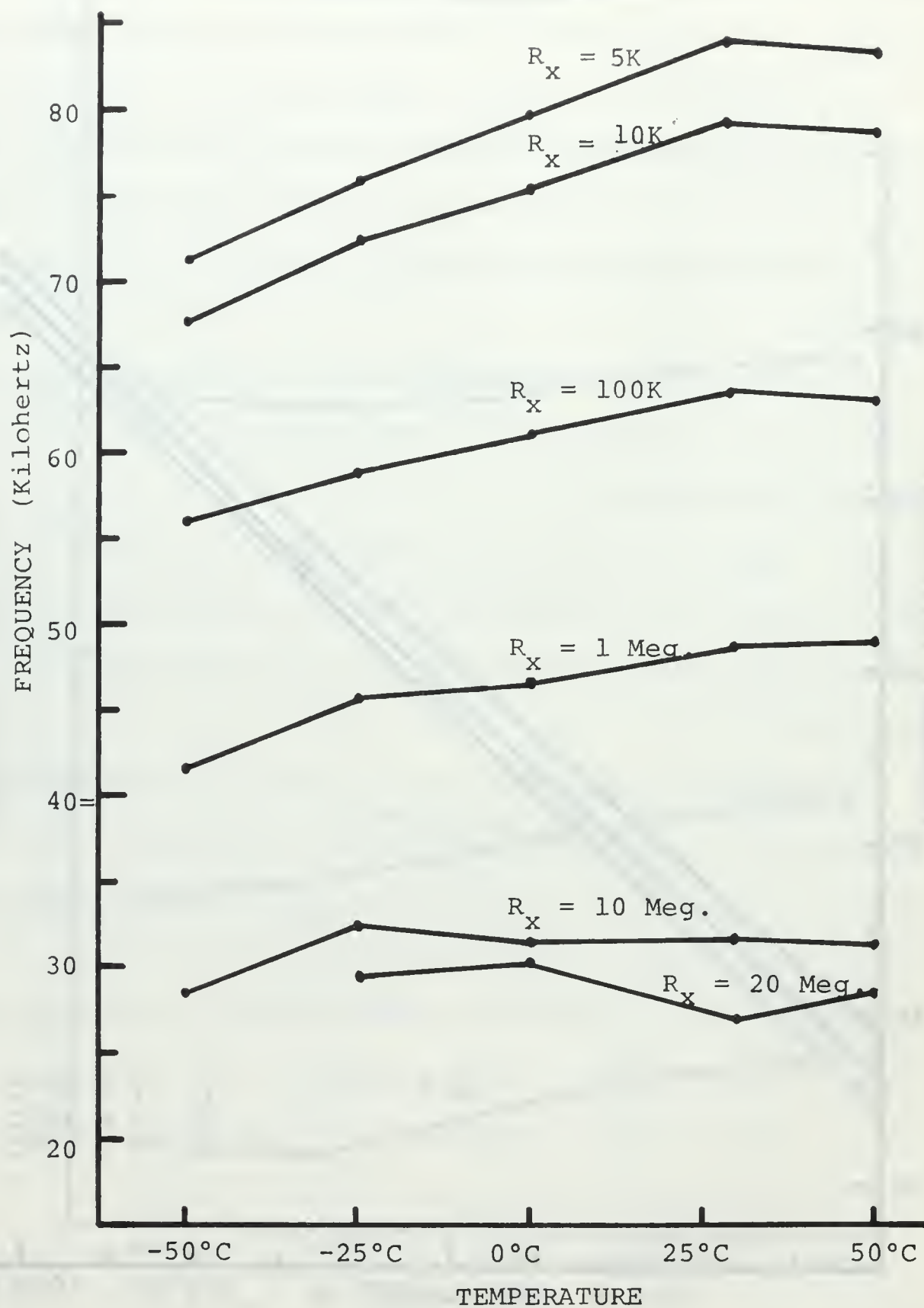


Figure 18. Humidity Channel Environmental Test VCM Frequency vs. Temperature.

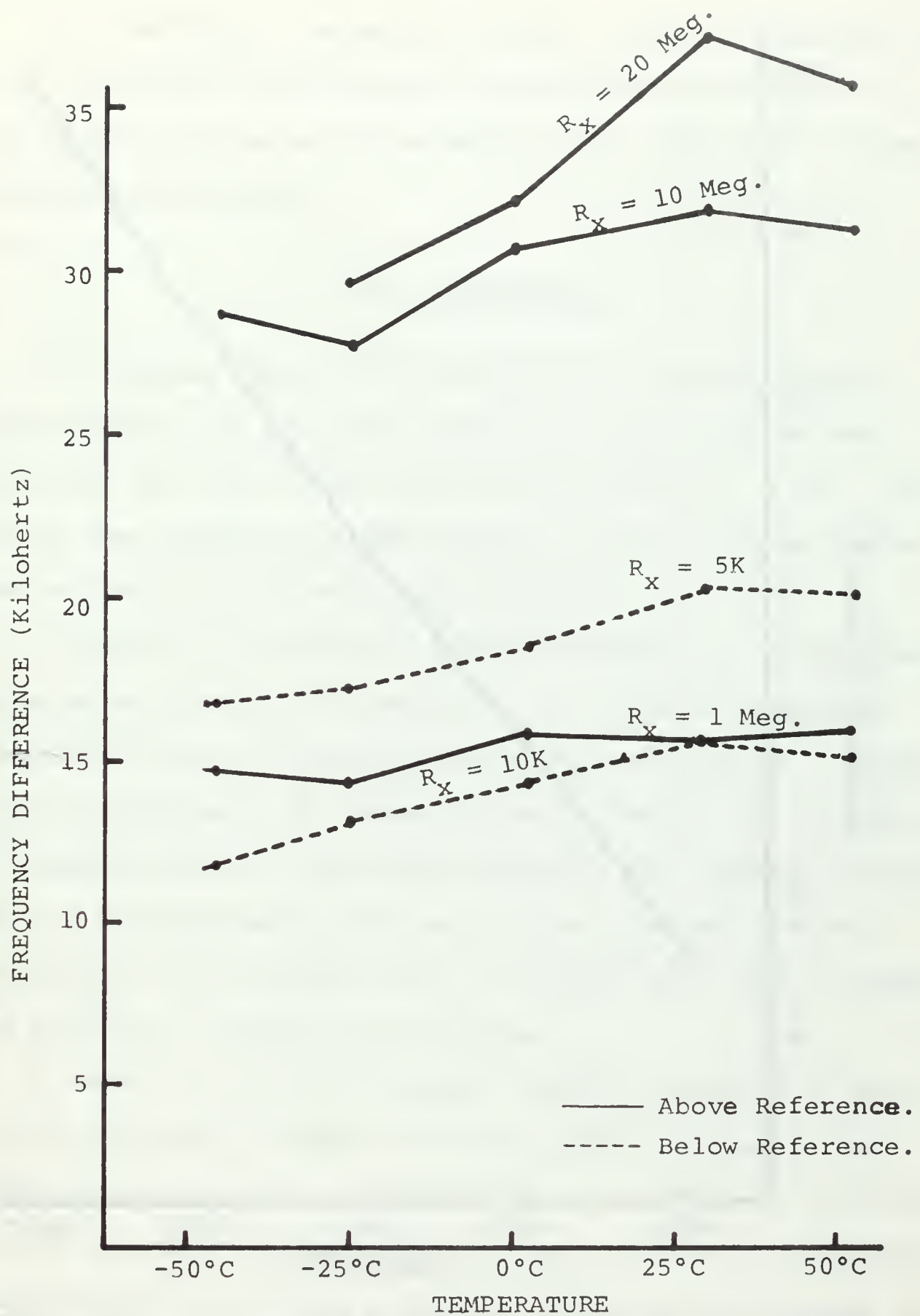


Figure 19. Humidity Channel Environmental Test Frequency Difference vs. Temperature.

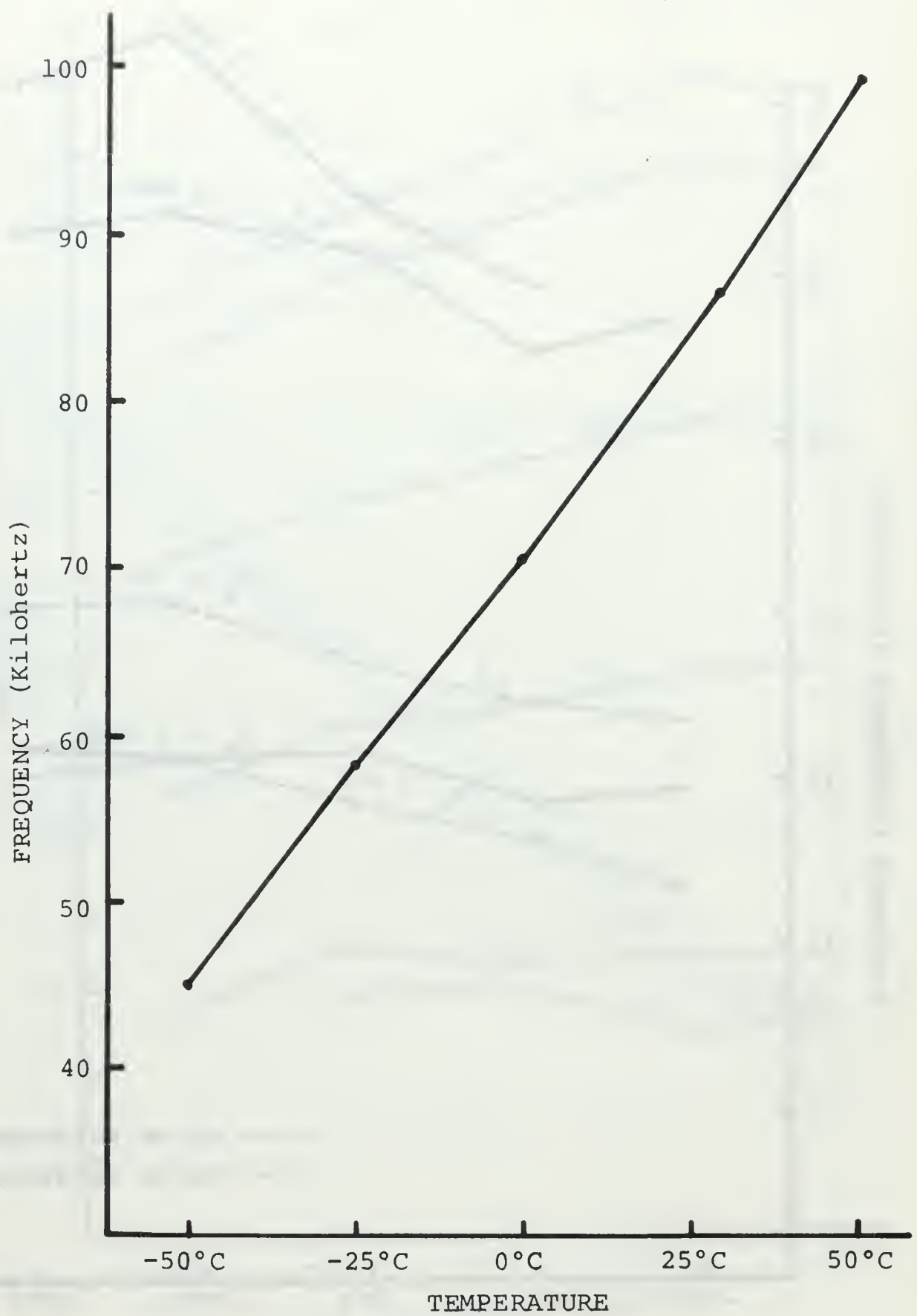


Figure 20. Temperature Channel Environmental Test VCM Frequency vs. Temperature.

2. The output frequencies of all interface channels vary over a somewhat larger range than originally specified. In all cases this can be corrected by small gain and/or offset-voltage adjustments.

V. CONCLUSION

This thesis dealt with the problem of converting the output signals of various sensors to a specified voltage variation for use as the controlling voltage of a VCM. The system was designed, breadboarded, and the complete system was subjected to an environmental test.

A system using state-of-the-art sensors and semiconductor integrated circuits is feasible. The interface circuits functioned over the range of temperatures required. Temperature coefficients of various circuit elements do contribute to nonlinearities in each data channel, but computer analysis of data should resolve the data to the accuracy desired. Meaningful data analysis must be delayed until final design and packaging studies are completed.

A solid-state pressure sensor which is capable of providing an output voltage over the ranges of pressure and temperatures required is available. A temperature coefficient exists and must be considered in data analysis. The passive compensation used in the prototype model tested will not give the accuracy specified in Table II.

Signal processing by diffused components was practiced in a rudimentary form by offsetting temperature-dependent

sensitivities with temperature-dependent gains in two of the data channels. This general form of processing could conceivably be used to decrease the temperature dependence of the VCM. The silicon chip used for the pressure transducer offers an area which could be used for the addition of diffused resistors, diodes, or transistors for this purpose.

The use of semiconductor junctions as temperature-sensing elements appears feasible. The accuracy and predictability of the junction voltage will finally determine the value of this measuring system.

Input bias requirements of the operational amplifiers used affected the performance of the interface circuits in several instances. A new generation of micropower operational amplifiers is becoming available, which not only have reduced bias requirements but have reduced power input requirements. Circuit modifications to permit use of these amplifiers would be desirable.

Minor design changes to the VCM and modulator section of the radiosonde should be made to improve the temperature dependence and standby power requirements. In the opinion of the author, the primary cause of frequency change with temperature is the change in base-emitter voltage of the current sources. Using negative-temperature-coefficient resistors in the emitters of this stage could decrease if not eliminate this characteristic. The modulator requires 40 milliamperes of standby current in this circuit. In a

circuit that depends on battery power, this is objectionable. It is believed that adding another buffer stage would decrease this current significantly.

The findings of this investigation appear to reinforce those of previous authors. Solid-state devices are available at reasonable costs which can be used for this application.

BIBLIOGRAPHY

1. Corbeille, R. C., An Experimental Investigation of Radiosondes, M.S. Thesis, Naval Postgraduate School, October, 1966.
2. Dowell, G. W., A Digital Radiosonde System, M.S. Thesis, Naval Postgraduate School, September 1967.
3. Sagerian, A., A Solid State Pulse Modulated Radiosonde, E.E. Thesis, Naval Postgraduate School, June 1969.
4. Newcomb, W., Sensors for Radiosonde Use, M.S. Thesis, Naval Postgraduate School, June 1969.
5. Jones, F. E., "Evaporated-Film Electric Hygrometer Elements," Journal of Research of the National Bureau
6. Application Brief, An Arithmetic Analog Computer Using the μ A735 Logarithmic Amplifiers, Fairchild Semiconductor, Inc.
7. Krasin, E. F., and Wood, K. J., An Advanced Meteorological Sounding System Design Plan, Motorola, Inc., Government Electronics Division, Contract No. AF 19(628)-4215, November 1965.
8. Griggs, W. M., and Wood, K. J., An Advanced Meteorological Sounding System, Phase II (Proof of Concept), Motorola, Inc., AFCRL-67-0268, Government Electronics Division, Contract No. AF 19(628)-4215, November 1965.

INITIAL DISTRIBUTION LIST

	No. Copies
1. Defense Documentation Center Cameron Station Alexandria, Virginia 22314	20
2. Library, Code 0212 Naval Postgraduate School Monterey, California	2
3. Commander, Naval Ordnance Systems Command Department of the Navy Washington, D. C. 20360	1
4. Assoc Professor R. Panholzer, Code 52 Pz Department of Electrical Engineering Naval Postgraduate School Monterey, California 93940	2
5. LCDR E. M. Hall P.O. Box 5 Oneonta, Alabama 35121	1

DOCUMENT CONTROL DATA - R & D

(Security classification of title, body of abstract and indexing annotation must be entered when the overall report is classified)

1. ORIGINATING ACTIVITY (Corporate author) Naval Postgraduate School Monterey, California 93940		2a. REPORT SECURITY CLASSIFICATION Unclassified	
		2b. GROUP	
3. REPORT TITLE A SENSOR INTERFACE SYSTEM FOR DIGITAL RADIOSONDES			
4. DESCRIPTIVE NOTES (Type of report and inclusive dates) Master's Thesis; December 1969			
5. AUTHOR(S) (First name, middle initial, last name) Eugene Mallory Hall Lieutenant Commander, United States Navy			
6. REPORT DATE December 1969		7a. TOTAL NO. OF PAGES 48	7b. NO. OF REFS
8a. CONTRACT OR GRANT NO.		9a. ORIGINATOR'S REPORT NUMBER(S)	
b. PROJECT NO.			
c.		9b. OTHER REPORT NO(S) (Any other numbers that may be assigned this report)	
d.			
10. DISTRIBUTION STATEMENT This document has been approved for public release and sale; its distribution is unlimited.			
11. SUPPLEMENTARY NOTES		12. SPONSORING MILITARY ACTIVITY Naval Postgraduate School Monterey, California 93940	
13. ABSTRACT A new radiosonde is needed to increase the accuracy, reliability, and speed of processing of upper-atmosphere observations. Two previous theses have investigated a pulse-modulated transmitter and more accurate sensors. This thesis proposes a method of combining the two into a workable radiosonde. Solid-state technology is used throughout including MOS integrated circuits, linear integrated circuits, and a silicon pressure transducer. System tests conducted under environmental conditions indicate satisfactory results.			

14

KEY WORDS

LINK A

LINK B

LINK C

ROLE

WT

ROLE

WT

ROLE

WT

Digital Radiosonde

Meteorological Sensor Interface

Silicon Bridge Pressure Transducer

thesH1475

A sensor interface system for digital ra



3 2768 001 01723 9

DUDLEY KNOX LIBRARY